Molecular Laser Cooling in a Dynamically Tunable Repulsive Optical Trap

Yukai Lu,[1,2] Connor M. Holland,[1] and Lawrence W. Cheuk[1]
[1]Department of Physics, Princeton University, Princeton, New Jersey 08544, USA
[2]Department of Electrical and Computer Engineering, Princeton University, Princeton, New Jersey 08544, USA

(Received 13 September 2021; revised 31 March 2022; accepted 3 May 2022; published 25 May 2022)

Recent work with laser-cooled molecules in attractive optical traps has shown that the differential ac Stark shifts arising from the trap light itself can become problematic, limiting collisional shielding efficiencies, rotational coherence times, and laser-cooling temperatures. In this Letter, we explore trapping and laser cooling of CaF molecules in a ring-shaped repulsive optical trap. The observed dependences of loss rates on temperature and barrier height show characteristic behavior of repulsive traps and indicate strongly suppressed average ac Stark shifts. Within the trap, we find that Λ-enhanced gray molasses cooling is effective, producing similar minimum temperatures as those obtained in free space. By combining in-trap laser cooling with dynamical reshaping of the trap, we also present a method that allows highly efficient and rapid transfer from molecular magneto-optical traps into conventional attractive optical traps, which has been an outstanding challenge for experiments to date. Notably, our method could allow nearly lossless transfer over millisecond timescales.

DOI: 10.1103/PhysRevLett.128.213201

Ultracold polar molecules, with their rich structure and long-range dipolar interactions, have been proposed as an ideal platform for applications ranging from quantum simulation and information processing to precision measurement [1–4]. These have led to many experimental efforts to produce, cool, and control molecules. Two approaches have been pursued intensely: coherent assembly from ultracold atoms and direct laser cooling. The first production of ground state molecules via coherent assembly [5] has led to recent work demonstrating quantum degeneracy of molecular gases [6–8]. With direct laser cooling, the first molecular magneto-optical traps (MOTs) [9–12] have paved the way towards laser cooling of a large variety of molecular species including polyatomic ones [13–18].

Many proposed applications require conservative trapping, motivating recent work on magnetic trapping [19] and optical trapping of molecules [20–22]. For laser-cooled molecules, attractive optical traps have been used so far, and in-trap sub-Doppler cooling has been shown to be somewhat effective. This has produced trapped samples of laser-cooled molecules with record phase-space densities and allowed their detection *in situ* [21–23]. Nevertheless, the light used to form an attractive optical trap can be problematic as it can cause rapid collisional loss through photoexcitation [24–26]. In addition, the ac Stark shifts that give rise to trapping are generically unequal for different internal states. These differential shifts have been found to affect in-trap laser cooling (to a larger extent for CaF than for YO) [21–23,27], rotational coherence times [28], and schemes to shield molecules from inelastic collisions [29]. Compared to attractive optical traps, repulsive optical traps largely avoid the above problems, since molecules preferentially avoid the trapping light.

In addition, repulsive traps could also allow production of large optically trapped samples crucial for many applications. In experiments to date, the trap volume mismatch between attractive optical traps (typically ∼100 μm due to limitations in laser power) and the initial MOTs (mm-sized) have limited transfer fractions to well below unity [21–23]. To address this issue, MOT compression by increasing magnetic field gradients alone [19], and compression in combination with laser-cooling [30], have been used to reduce the initial size. Repulsive optical traps offer a new species-independent approach that provides much larger trap volumes. While an attractive trap requires optical power that scales with the cross-sectional area of the trap, for a ring-shaped repulsive trap, the required power scales only with the trap circumference.

These two advantages, suppressed Stark shifts and larger trap volumes, motivate us to explore repulsive optical potentials for molecules. In this Letter, we demonstrate 2D trapping and laser cooling of CaF molecules in a near-detuned repulsive optical barrier. In addition, by using a dynamically reshaped repulsive trap as an intermediary step, we demonstrate a new method to transfer molecules into an attractive optical dipole trap with record speed and efficiency.

Our starting point is a Λ-cooled cloud of CaF molecules in the $|X, v = 0, N = 1\rangle$ rotational manifold at zero magnetic field [31]. In brief, a DC-MOT [34] of CaF molecules is loaded from a cryogenic buffer gas beam (CBGB) [32] slowed via chirped slowing [35,36]. Subsequently, the MOT is compressed and released in the presence of

Λ-cooling light for 10 ms. The Λ-cooled cloud has a Gaussian diameter (2σ) of 1.2(1) mm and consists of 4.5×10^4 molecules at a temperature of ∼10 μK.

The repulsive optical trap is ring shaped and formed with light blue-detuned by $\Delta_t = 108$ GHz from the $X^2\Sigma^+(v=0,N=1) \rightarrow B^2\Sigma^+(v=0,N=0)$ transition. The ring radius is dynamically tunable over ms timescales [31]. To a good approximation, the potential is axially invariant in the region explored by the molecules [31]. In addition, the lack of thermalization over the explored timescales implies that the system is effectively two-dimensional. Since the molecular temperature k_BT is much lower than the barrier height U_0, the potential explored by the molecules is well approximated by

$$U(\mathbf{r}) = \begin{cases} 0, & r \le r_0 \\ a(r-r_0)^\alpha, & r > r_0, \end{cases} \quad (1)$$

where $\alpha \gg 1$ [Fig. 1(c)].

In optical traps, undesirable effects such as differential ac Stark shifts and heating are proportional to the trap light intensity. Since the off-resonant photon scattering rate is also proportional to the light intensity, one can use the trap-averaged photon scattering rate $\langle\Gamma_{sc}\rangle_{trap}$ as a figure of merit. For a thermal ensemble in an attractive trap, $\langle\Gamma_{sc}\rangle_{trap} \propto V$, where V is the trap depth. In contrast, for a repulsive trap, the scaling of $\langle\Gamma_{sc}\rangle_{trap}$ with barrier height is geometry-dependent. For the ring-shaped barrier explored here, $\langle\Gamma_{sc}\rangle_{trap}$ is approximately linear with T and independent of barrier height:

$$\langle\Gamma_{sc}\rangle_{trap} \propto \frac{\int d\mathbf{r} U(\mathbf{r}) e^{-U(\mathbf{r})/(k_BT)}}{\int d\mathbf{r} e^{-U(\mathbf{r})/(k_BT)}} \propto T\left(\frac{T}{a}\right)^{\mathcal{O}(1/\alpha)}. \quad (2)$$

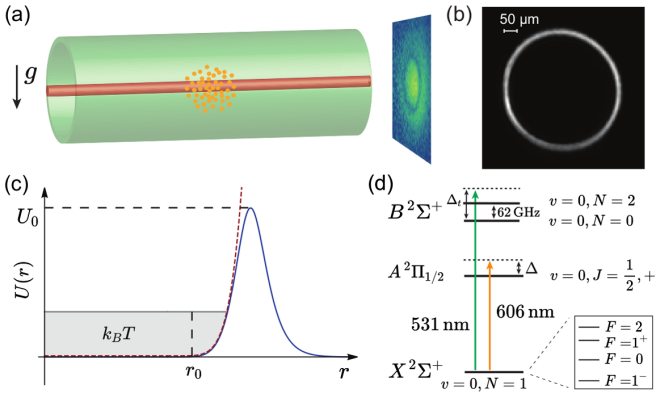

FIG. 1. (a) Experimental setup. A ring-shaped repulsive trap (green) runs concentrically with an attractive optical dipole trap (red) formed from a focused Gaussian beam. Molecules are detected by imaging along the same axis. (b) Intensity distribution of the repulsive trap [$r_0 = 160(10)$ μm]. (c) Model potential for the ring trap. (d) Energy level diagram of CaF with relevant transitions.

Consequently, at low temperatures, photon scattering and therefore differential ac Stark shifts are strongly suppressed. Similar scaling laws for other trap geometries have been derived in previous work with ultracold atoms [37].

To observe the trap depth and temperature scalings predicted by Eq. (2), we characterize trap heating and loss rates, which act as probes for $\langle\Gamma_{sc}\rangle_{trap}$. Molecules are transferred from the Λ-cooled cloud into a conventional attractive optical dipole trap (ODT) concentric with the ring trap. The ODT is generated using a laser beam at 1064 nm focused to a Gaussian waist of 60(7) μm, much smaller than the repulsive ring radius, and retroreflected to form a 1D lattice [Fig. 1(a)]. Subsequently, the cooling light is switched off and untrapped molecules fall away over 50 ms. The molecules are then released into the repulsive ring trap, which has radius $r_0 = 160(10)$ μm and a barrier height of $U_0/k_B = 240(30)$ μK. A 2 ms Λ-cooling pulse then recools the cloud to 10(1) μK. The number and the temperature T are then measured as a function of the hold time in the trap. The measurements yield a $1/e$ lifetime of 46(4) ms, with no observable temperature increase [Figs. 2(a) and 2(b)].

At first sight, the lack of significant heating seems to contradict Eq. (2), which predicts $\dot{T} \propto T$ and hence exponentially increasing temperatures. The observation of strong losses with minimal heating can be explained by loss to undetected rotational states resulting from Raman scattering. Specifically, molecules off-resonantly excited to $|B, v=0, N=0\rangle$ always return to $|X, v=0, N=1\rangle$ and experience recoil heating, but molecules excited to $|B, v=0, N=2\rangle$ are lost from detection if they decay to $|X, v=0, N=3\rangle$. One therefore expects a rotational loss rate on the order of $\langle\Gamma_{sc}\rangle_{trap}$. On the other hand, off-resonant scattering imparts kinetic energy at a rate of $\sim\langle\Gamma_{sc}\rangle_{trap} E_R$, where $E_R = \hbar^2k^2/(2m) = k_B \times 0.58$ μK is the recoil

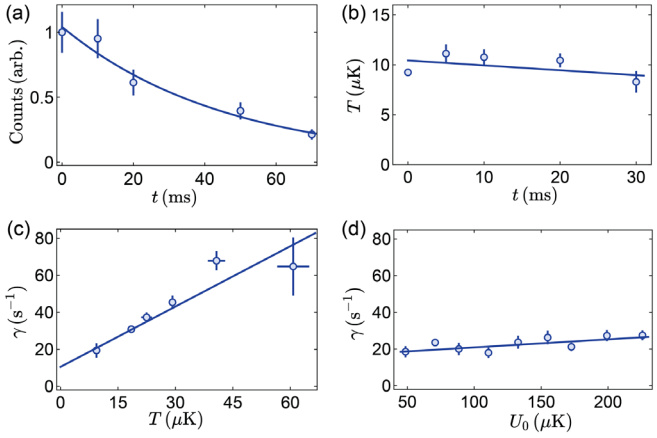

FIG. 2. (a) Normalized molecular number N versus hold time t. An exponential fit (solid) yields a $1/e$ time of 46(4) ms. (b) Temperature T versus hold time t. (c) Loss rate γ versus temperature T. (d) Loss rate versus barrier height U_0. For (b),(c), (d), solid lines show linear fits.

energy, and k is the trapping light wave vector. Since the initial temperature (10 μK) is well above E_R/k_B, molecules are rotationally lost before significant heating occurs. This is true in far-detuned optical traps when temperatures are well above E_R/k_B, a regime reached in many laser-cooling experiments. We note that additional rotational repumpers could suppress these losses and allow observation of exponential heating.

The molecular loss rate is therefore a good proxy for the average scattering rate $\langle\Gamma_{sc}\rangle_{trap}$, and should scale linearly with T and be independent of U_0 according to Eq. (2). To observe the temperature dependence, we vary the molecular temperature between 9.4(3) and 61(4) μK by adjusting the cooling parameters of the 2 ms Λ-cooling pulse applied following trap loading. Indeed, we find that the $1/e$ loss rate γ increases linearly with T with an offset at $T = 0$ [Fig. 2(c)]. The $T = 0$ offset could arise from residual light on the interior of the ring, imperfect ring sharpness, and other loss mechanisms such as collisions with background gas. We note that the observed loss rates are $\sim 10^{-2}\Gamma_{sc,max}$, where $\Gamma_{sc,max}$ is the theoretically predicted loss rate at the peak barrier intensity [31]. Noting that the trap-averaged ac Stark shifts are proportional to $\langle\Gamma_{sc}\rangle_{trap}$, our observations therefore show that ac Stark shifts are also strongly suppressed compared to an attractive trap with a similar depth and absolute polarizability.

We next probe the dependence of $\langle\Gamma_{sc}\rangle_{trap}$ on barrier height U_0. Starting with molecules at $10(1)$ μK, we abruptly change the barrier height U_0/k_B to a value between 50 and 230 μK. As shown in Fig. 2(d), the loss rates are found to increase slightly with U_0. This generally agrees with Eq. (2), which predicts γ to be largely independent of U_0, in contrast to the linear scaling for attractive traps ($\gamma \propto V$). The small increase in loss rate with U_0 likely arises from residual light within the ring.

Having explored the dependences of loss and heating on T and U_0, we next investigate laser cooling, specifically Λ cooling, in the repulsive trap. In attractive optical traps, differential ac Stark shifts could affect the effectiveness of Λ cooling by destabilizing the coherent dark states involved. Degradation of laser cooling in optical traps has been observed for CaF [23], while for YO, this effect has been found to be minimal [22]. In repulsive traps, one could expect in-trap laser cooling to perform similarly as in free space, since the molecules avoid the trapping light. Although one expects laser cooling to be effective on timescales shorter than the transit time τ_t of a molecule across the trap ($\tau_t = r_0/\sqrt{2k_BT/m} \approx 1$–$3$ ms), on longer timescales, the effectiveness of in-trap Λ cooling could be affected as molecules are reflected by the repulsive potential. Several mechanisms can lead to heating and loss. First, molecules in the excited state could experience opposite ac Stark shifts and become untrapped or experience heating near the ring. Second, strong differential Stark shifts could convert Λ cooling into Λ heating [22]. These are particularly strong in our case since the trap light is only detuned by a few rotational constants ($\Delta_t \approx 5B$, where $B \approx 20$ GHz is the rotational constant). Third, multiphoton processes involving the trap light in combination with the cooling light can also lead to heating.

To characterize in-trap Λ cooling, we compare temperatures obtained in free space to those obtained in-trap following identical laser-cooling pulses. Molecules are loaded from the Λ-cooled cloud into the ring trap by suddenly switching the trap on, which ensures that the in-ring molecules are in contact with the repulsive light. Subsequently, we wait 30 ms for untrapped molecules to fall away. A 5 ms Λ-cooling pulse with various detunings Δ and intensities I is then applied, both with or without the ring present. Over the explored range of Λ-cooling parameters, we observe no significant difference between temperatures obtained in-trap (T_R) and those obtained in free space (T_{FS}) [Fig. 3(a)]. Notably, the minimum temperature reached in the trap is similar to that obtained in free space. To investigate whether additional heating processes involving trap light are present, we plot the ratio $\kappa = T_R/T_{FS}$ versus the cooling light intensity I [Fig. 3(b)]. We observe no dependence of κ on I, which rules out significant heating processes involving both cooling and trapping light, since an incoherent process with n photons of cooling light would show an I^n dependence.

We next examine whether laser cooling leads to additional losses for the trapped molecules. We compare the $1/e$ lifetimes τ of the trapped molecules with and without Λ-cooling light, and find $\tau = 57(1)$ and $\tau = 40(1)$ ms, respectively. These are much longer than the transit time τ_t, which indicate that in-trap cooling does not lead to additional losses compared to trapping alone. We note in passing that we obtain lifetimes up to 100 ms when the repulsive barrier light is further detuned [31].

Next, we illustrate how the large volume available with our repulsive ring trap enables efficient transfer of molecules from a MOT. We first set the ring radius to

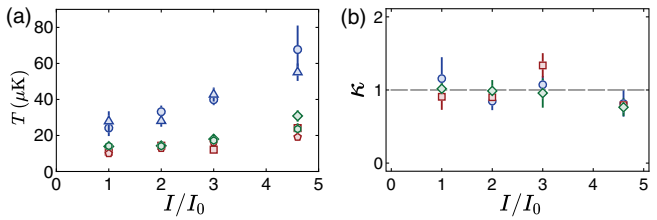

FIG. 3. (a) Temperature versus cooling light intensity I/I_0 at various Λ-cooling light detunings Δ, in free space and in trap. Blue circles, green diamonds, and red squares show free space temperatures; Blue triangles, green pentagons, and red hexagons show in-trap temperatures. (b) Ratio of the in-trap to free-space temperature κ versus cooling light intensity I/I_0. For both plots, I is the single-beam single-axis intensity, $I_0 = 5.0(5)$ mW/cm^2; $\Delta = 6$ MHz (blue circles, triangles), 13 MHz (green diamonds, pentagons), and 38 MHz (red squares, hexagons).

$r_0 = 414(2)$ μm [barrier height $U_i/k_B = 65(1)$ μK] to maximize the spatial overlap with the Λ-cooled cloud, whose size is similar to that of the MOT. The ring trap is then switched on following initial Λ cooling, after which we wait 21 ms for any transient dynamics to damp out. We subsequently image the molecular cloud *in situ* using a 250 μs pulse of resonant light. Despite blurring during imaging [31], we observe a clear boundary between trapped and untrapped molecules, and find that 27(3)% is captured into the repulsive trap [Fig. 4(b)]. This improves upon past experiments with attractive optical traps, where the size mismatch with the initial MOTs has limited transfer efficiencies to ~5% [21,23,30].

Although the ring-shaped trap offers large trap volumes with limited laser power, it has a drawback. For a fixed molecule number, in-trap laser cooling produces negligible density enhancement, unlike in a Gaussian-shaped attractive trap where density can be strongly enhanced at lower temperatures [20–23]. To benefit from both the large capture volume of the repulsive trap and the density enhancement offered by a conventional attractive trap, we have developed the following two-step transfer procedure. After initial capture into the large volume ring trap, we dynamically reduce the ring size while applying laser cooling. The compressed cloud is subsequently transferred into an attractive ODT in the presence of Λ cooling. This two-step procedure allows much better mode matching both with the MOT and the attractive trap, resulting in improved overall transfer efficiencies.

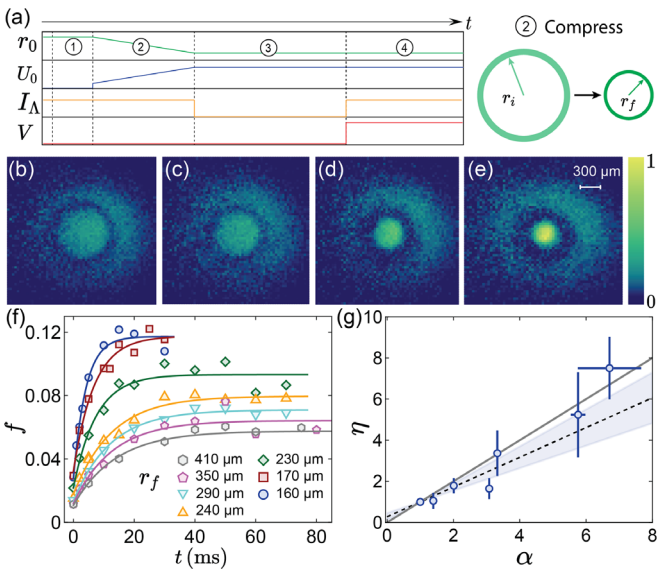

FIG. 4. (a) Experimental sequence for enhanced transfer into an attractive ODT: (i) free-space cooling (10 ms), (ii) compression with cooling (21 ms), (iii) release of untrapped molecules (30 ms), and (iv) transfer into the attractive ODT with cooling. Shown are the ring radius r_0, barrier height U_0, cooling light intensity I, and attractive ODT depth V versus time. (b),(c),(d),(e) *In situ* images during compression, taken 0, 6, 15, 21 ms, into the ramp, respectively. (f) Transfer fraction f versus loading time t. Solid lines are fits to an exponential saturation curve. (g) Loading rate enhancement η versus compression ratio $\alpha = r_i^2/r_f^2$. Solid line shows the expected geometric enhancement $\eta = \alpha$. Dashed line shows a linear fit to data with $\eta = \alpha = 1$ fixed. The shaded region indicates $\pm 1\sigma$ bands for the fit.

In detail, the repulsive ring has an initial radius of $r_i = 414(2)$ μm and barrier height of $U_i/k_B = 65(1)$ μK. Over the next 21 ms, the radius is smoothly reduced to $r_f = 160(10)$ μm and the barrier height is increased to $U_f/k_B = 240(30)$ μK [Fig. 4(a)] [31]. *In situ* images show rising densities throughout compression [Figs. 4(b)–4(e)]. T is found to remain constant at the initial temperature $T_i \approx 10$ μK [31], indicating sufficient cooling. In the absence of cooling, compression-induced heating would produce a final temperature $T_f \geq \alpha T_i$, where $\alpha = r_i^2/r(t)^2$ is the compression ratio and the lower bound assumes adiabaticity.

To transfer molecules from the repulsive trap into the much smaller attractive ODT, we switch on the attractive trap in the presence of Λ-cooling light. Figure 4(f) shows the transfer fraction $f = N_{\mathrm{ODT}}/N_{\mathrm{SD}}$ versus transfer time t, where N_{SD} is the initial number in the Λ-cooled cloud. The transfer fraction initially rises and then saturates, with both the loading rate and the saturated transfer fraction increasing with compression. Since the initial loading rate $R_0 = \dot{N}_{\mathrm{ODT}}(t=0)/N_{\mathrm{SD}}$ is proportional to the initial density, the normalized initial loading rate $\eta = R_0(\alpha)/R_0(\alpha = 1)$ directly measures the density enhancement. As shown in Fig. 4(g), we observe a peak enhancement factor of 6 and find that $\eta \approx \alpha$, consistent with the geometric expectation from the reduced ring area. At maximum compression ($\alpha \approx 6$), rapid saturation times around 10 ms are observed, much faster than the ~100 ms times previously reported [21–23]. We also observe highly efficient transfer, with 45(5)% of the repulsively trapped molecules transferred into the attractive ODT. This corresponds to an overall transfer efficiency of 12(2)% from the Λ-cooled cloud, with $5.4(5) \times 10^3$ molecules trapped in the ODT.

Although the loading rate is enhanced sixfold by trap compression, the final trapped number is enhanced only twofold. We believe that this is limited by the initial number captured into the repulsive trap, since the transfer fraction from repulsive to attractive trap is consistent with the measured lifetimes. This can be improved with a faster compression rate, which we find can be as fast as the cooling rate $\dot{T}/T$ [31]. Based on the observed and theoretically predicted sub-Doppler cooling timescales of ≈100 μs [20,30,38,39], sub-ms-scale compression, much faster than the 21 ms used here, could further improve transfer efficiencies.

In conclusion, we have explored trapping and laser cooling of molecules in a near-detuned repulsive optical trap. We have observed temperature and power dependences consistent with strongly suppressed photon scattering rates, and found that in-trap Λ cooling performs similarly as

in free space. By combining laser cooling with dynamical reshaping of a repulsive trap, we have also demonstrated a new species-independent method to rapidly transfer laser-cooled molecules into optical traps with record efficiencies. This paves the way for near lossless transfer from MOTs into optical traps, overcoming an outstanding experimental challenge.

Looking ahead, laser cooling in dynamically tunable repulsive traps could be widely applicable in future explorations with laser-cooled molecules. For evaporative cooling, collisional shielding could be more effective due to suppressed differential Stark shifts [29] and dynamical compression could offer high densities. Repulsive bottle-beam optical tweezers [40] could provide lower decoherence rates for molecular qubits [28]. For precision measurement with trapped laser-cooled molecules [4], repulsive ring traps could suppress effects from trap inhomogeneity, and dynamic decompression could lower temperatures and densities, reducing systematics from Doppler shifts and molecular interactions.

Y. L. and C. M. H. contributed equally to this work.

[1] L. D. Carr, D. DeMille, R. V. Krems, and J. Ye, New J. Phys. **11**, 055049 (2009).

[2] J. L. Bohn, A. M. Rey, and J. Ye, Science **357**, 1002 (2017).

[3] J. A. Blackmore, L. Caldwell, P. D. Gregory, E. M. Bridge, R. Sawant, J. Aldegunde, J. Mur-Petit, D. Jaksch, J. M. Hutson, B. E. Sauer, M. R. Tarbutt, and S. L. Cornish, Quantum Sci. Technol. **4**, 014010 (2018).

[4] B. L. Augenbraun, Z. D. Lasner, A. Frenett, H. Sawaoka, C. Miller, T. C. Steimle, and J. M. Doyle, New J. Phys. **22**, 022003 (2020).

[5] K.-K. Ni, S. Ospelkaus, M. H. G. de Miranda, A. Pe'er, B. Neyenhuis, J. J. Zirbel, S. Kotochigova, P. S. Julienne, D. S. Jin, and J. Ye, Science **322**, 231 (2008).

[6] L. De Marco, G. Valtolina, K. Matsuda, W. G. Tobias, J. P. Covey, and J. Ye, Science **363**, 853 (2019).

[7] M. Duda, X.-Y. Chen, A. Schindewolf, R. Bause, J. von Milczewski, R. Schmidt, I. Bloch, and X.-Y. Luo, Transition from a polaronic condensate to a degenerate fermi gas of heteronuclear molecules, arXiv:2111.04301.

[8] A. Schindewolf, R. Bause, X.-Y. Chen, M. Duda, T. Karman, I. Bloch, and X.-Y. Luo, Evaporation of microwave-shielded polar molecules to quantum degeneracy, arXiv:2201.05143.

[9] J. F. Barry, D. J. McCarron, E. B. Norrgard, M. H. Steinecker, and D. DeMille, Nature (London) **512**, 286 (2014).

[10] S. Truppe, H. J. Williams, M. Hambach, L. Caldwell, N. J. Fitch, E. A. Hinds, B. E. Sauer, and M. R. Tarbutt, Nat. Phys. **13**, 1173 (2017).

[11] L. Anderegg, B. L. Augenbraun, E. Chae, B. Hemmerling, N. R. Hutzler, A. Ravi, A. Collopy, J. Ye, W. Ketterle, and J. M. Doyle, Phys. Rev. Lett. **119**, 103201 (2017).

[12] A. L. Collopy, S. Ding, Y. Wu, I. A. Finneran, L. Anderegg, B. L. Augenbraun, J. M. Doyle, and J. Ye, Phys. Rev. Lett. **121**, 213201 (2018).

[13] I. Kozyryev, L. Baum, K. Matsuda, B. L. Augenbraun, L. Anderegg, A. P. Sedlack, and J. M. Doyle, Phys. Rev. Lett. **118**, 173201 (2017).

[14] J. Lim, J. R. Almond, M. A. Trigatzis, J. A. Devlin, N. J. Fitch, B. E. Sauer, M. R. Tarbutt, and E. A. Hinds, Phys. Rev. Lett. **120**, 123201 (2018).

[15] D. Mitra, N. B. Vilas, C. Hallas, L. Anderegg, B. L. Augenbraun, L. Baum, C. Miller, S. Raval, and J. M. Doyle, Science **369**, 1366 (2020).

[16] B. L. Augenbraun, J. M. Doyle, T. Zelevinsky, and I. Kozyryev, Phys. Rev. X **10**, 031022 (2020).

[17] L. Baum, N. B. Vilas, C. Hallas, B. L. Augenbraun, S. Raval, D. Mitra, and J. M. Doyle, Phys. Rev. A **103**, 043111 (2021).

[18] X. Alauze, J. Lim, M. Trigatzis, S. Swarbrick, F. Collings, N. Fitch, B. Sauer, and M. Tarbutt, Quantum Sci. Technol. **6**, 044005 (2021).

[19] H. J. Williams, L. Caldwell, N. J. Fitch, S. Truppe, J. Rodewald, E. A. Hinds, B. E. Sauer, and M. R. Tarbutt, Phys. Rev. Lett. **120**, 163201 (2018).

[20] L. Anderegg, B. L. Augenbraun, Y. Bao, S. Burchesky, L. W. Cheuk, W. Ketterle, and J. M. Doyle, Nat. Phys. **14**, 890 (2018).

[21] T. K. Langin, V. Jorapur, Y. Zhu, Q. Wang, and D. DeMille, Phys. Rev. Lett. **127**, 163201 (2021).

[22] Y. Wu, J. J. Burau, K. Mehling, J. Ye, and S. Ding, Phys. Rev. Lett. **127**, 263201 (2021).

[23] L. W. Cheuk, L. Anderegg, B. L. Augenbraun, Y. Bao, S. Burchesky, W. Ketterle, and J. M. Doyle, Phys. Rev. Lett. **121**, 083201 (2018).

[24] A. Christianen, M. W. Zwierlein, G. C. Groenenboom, and T. Karman, Phys. Rev. Lett. **123**, 123402 (2019).

[25] P. D. Gregory, J. A. Blackmore, S. L. Bromley, and S. L. Cornish, Phys. Rev. Lett. **124**, 163402 (2020).

[26] R. Bause, A. Schindewolf, R. Tao, M. Duda, X.-Y. Chen, G. Quéméner, T. Karman, A. Christianen, I. Bloch, and X.-Y. Luo, Phys. Rev. Research **3**, 033013 (2021).

[27] L. Caldwell and M. R. Tarbutt, Phys. Rev. Research **2**, 013251 (2020).

[28] S. Burchesky, L. Anderegg, Y. Bao, S. S. Yu, E. Chae, W. Ketterle, K.-K. Ni, and J. M. Doyle, Phys. Rev. Lett. **127**, 123202 (2021).

[29] L. Anderegg, S. Burchesky, Y. Bao, S. S. Yu, T. Karman, E. Chae, K.-K. Ni, W. Ketterle, and J. M. Doyle, Science **373**, 779 (2021).

[30] S. Ding, Y. Wu, I. A. Finneran, J. J. Burau, and J. Ye, Phys. Rev. X **10**, 021049 (2020).

[31] See Supplemental Material at http://link.aps.org/supplemental/10.1103/PhysRevLett.128.213201 for details of the experimental apparatus and the data analysis, which contains Refs. [32,33].

[32] N. R. Hutzler, H.-I. Lu, and J. M. Doyle, Chem. Rev. **112**, 4803 (2012).

[33] L. W. Cheuk, L. Anderegg, Y. Bao, S. Burchesky, S. S. Yu, W. Ketterle, K.-K. Ni, and J. M. Doyle, Phys. Rev. Lett. **125**, 043401 (2020).

[34] M. R. Tarbutt and T. C. Steimle, Phys. Rev. A **92**, 053401 (2015).

[35] S. Truppe, H. J. Williams, N. J. Fitch, M. Hambach, T. E. Wall, E. A. Hinds, B. E. Sauer, and M. R. Tarbutt, New J. Phys. **19**, 022001 (2017).
[36] C. M. Holland, Y. Lu, and L. W. Cheuk, New J. Phys. **23**, 033028 (2021).
[37] N. Friedman, A. Kaplan, and N. Davidson, Adv. At. Mol. Opt. Phys. **48**, 99 (2002).
[38] J. Devlin and M. Tarbutt, New J. Phys. **18**, 123017 (2016).
[39] L. Caldwell, J. A. Devlin, H. J. Williams, N. J. Fitch, E. A. Hinds, B. E. Sauer, and M. R. Tarbutt, Phys. Rev. Lett. **123**, 033202 (2019).
[40] D. Barredo, V. Lienhard, P. Scholl, S. de Léséleuc, T. Boulier, A. Browaeys, and T. Lahaye, Phys. Rev. Lett. **124**, 023201 (2020).